JOURNAL OF MATERIALS SCIENCE 27 (1992) 1375–1379

Microstructural development in microsecond pulsed laser melted polycrystalline nickel

V. T. SWAMY, S. RANGANATHAN, K. CHATTOPADHYAY
Department of Metallurgy, Indian Institute of Science, Bangalore 560012, India

The microsecond Nd glass pulsed laser interaction with polycrystalline nickel was studied with particular emphasis on melting and the nature of the microstructural development following irradiation. The change in the melt pool shape and the melting efficiency as a function of the total laser power has been determined. Evidence is presented to show that for low energy pulse, the microstructural development accompanies fresh nucleation of grains and leads to a finer grain size than that of the substrate. At a higher energy level, growth competition leads to a coarser grain size. We also report a banded feature roughly parallel to the melt substrate interface that develops in the resolidified region during high energy interaction. These results are discussed in the light of our present understanding of rapid solidification processes.

1. Introduction

Solidification involves the nucleation and growth of solid phases from the liquid. The relative importance of these two processes often controls the resultant solidification microstructure. During the resolidification of a laser melted pool of metals and alloys, a substrate is always in contact with the melt. This often eliminates the need for nucleation. As a result, epitaxial regrowth is the dominant solidification mechanism during laser processing of single crystals of metals. The experiments by Buene *et al.* [1] on a single crystal of nickel confirms this conclusion. However, the situation can be different for a polycrystalline substrate. In this case, the crystals or grains in contact with the liquid pool will have different crystallographic orientations with respect to the melt–solid interface. The heat transfer direction on the other hand is generally normal to the melt–solid interface. This may lead to a growth competition between different grains. Such a growth competition favours a coarsening of the polycrystalline grains [2], because the unfavourably oriented grains will get eliminated during the growth process. On the other hand, the inhibition to growth due to the crystallographic factor may promote interface undercooling in a high heat transfer situation and incite fresh nucleation of the favourably oriented crystals at the interface. For such a case, a refinement of the structure will be observed in the resolidified microstructure. In this paper we report the results of laser experiments on polycrystalline nickel designed to understand the melting and microstructural evolution prior to the onset of drilling process. The material used contains impurities as follows: 0.12% Fe, 0.085% Co and 0.012% Mn (in wt %). Although this modifies the growth situation, it also acts as a marker to reveal the early stages of microstructural development during solidification of the laser melted pool.

2. Experimental procedure

A Nd glass pulsed laser with 200 μs pulsing time was used for the present experiment [3]. The laser has a triangular temporal profile with a peak power at 50 μs. The nickel specimens were optically polished before irradiation. Although this reduces the coupling efficiency, it ensures a standard surface state. During each experiment, the total energy of the laser pulse was carefully measured for the same settings prior to the laser processing of our samples. Measuring the energy density (fluence) for a beam with Gaussian spatial and triangular temporal profile is more difficult. An average fluence is, however, determined, assuming a beam diameter of 0.664 cm (diameter of smallest clean drill hole) strictly for comparison purposes. The irradiated portions were carefully sectioned and etched to reveal the cross-sectional microstructure. A JSM 840 scanning electron microscope was used for microstructural observation.

3. Results and discussion

Fig. 1 shows the radius of the laser affected region at the surface of the substrate as a function of total energy. The cross-sectional profiles of representative regions of the four points marked in Fig. 1 are shown in Fig. 2. An examination of the cross-sectional profiles indicates that at a lower power level away from the nose, the melt cavity approximates a section of a sphere. However, at a higher energy near the nose, the melt pool penetrates further inside the substrate and the melt pool profile changes to a parabolic shape. Following this, metal removal occurs leading to the onset of drilling and corresponds to regions near the nose of the plot in Fig. 1.

The experimentally determined surface and cross-sectional profiles at each energy level permits us to model the three-dimensional shape and volume of the

0022–2461

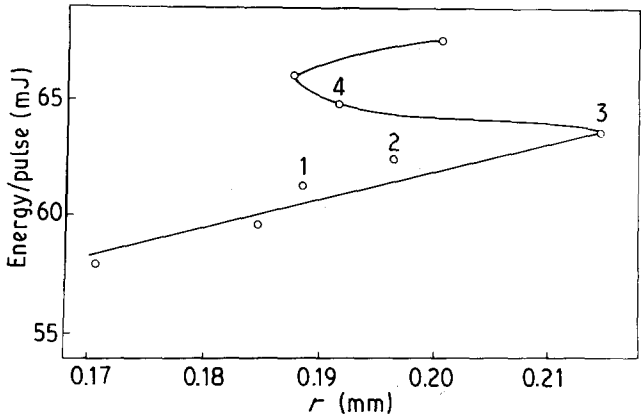

Figure 1 Radius of the irradiated spots at the substrate surface versus total energy per pulse for nickel.

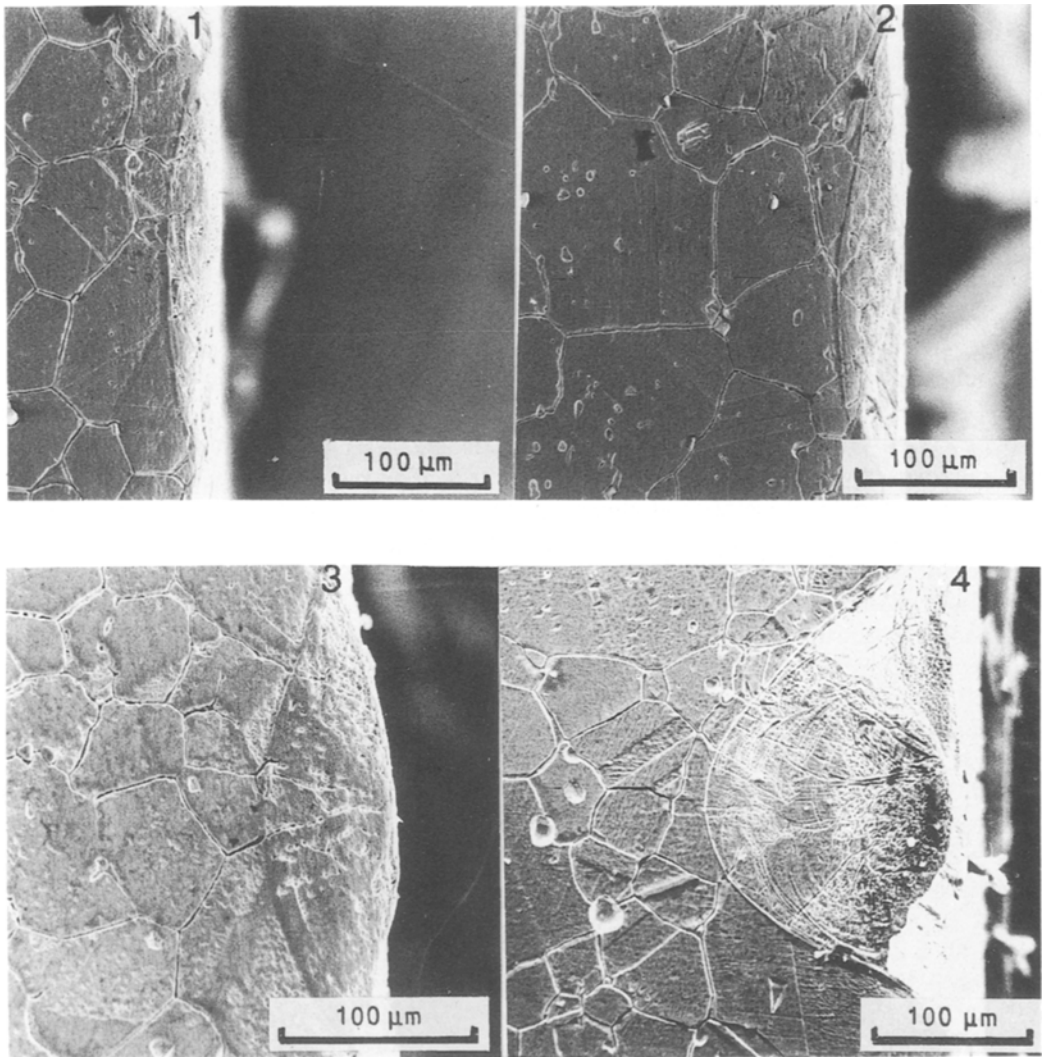

Figure 2 Cross-sectional profile of laser melted pool corresponding to points 1–4 in Fig. 1.

laser affected region. This allows us to determine melting efficiency defined as the ratio of the required thermal energy to melt the given volume of nickel to the total energy supplied by the laser. Fig. 3 shows a plot of melting efficiency as a function of total energy per pulse. As can be seen, the efficiency increases significantly within a narrow energy range indicating a band of critical threshold for such a change (corresponding to the regions near the nose of Fig. 1). Microstructurally this approximately corresponds to the change from a spherical to a parabolic profile and probably marks the onset of the keyhole effect of increased energy absorption discussed by several investigators [4–6].

Fig. 4a and b show low and high magnification micrographs, revealing the nature of the microstructure in the resolidified regions having the parabolic cross-sectional characteristic of relatively higher energy level per pulse irradiation (fluence 14.41 J cm^{-2}).

The temperature gradient in the liquid is steepest under this condition due to the fact that surface of the melt now approaches the evaporation threshold. The average grain size of the substrate is ~ 50 μm. The epitaxial regrowth of the grains into the resolidified

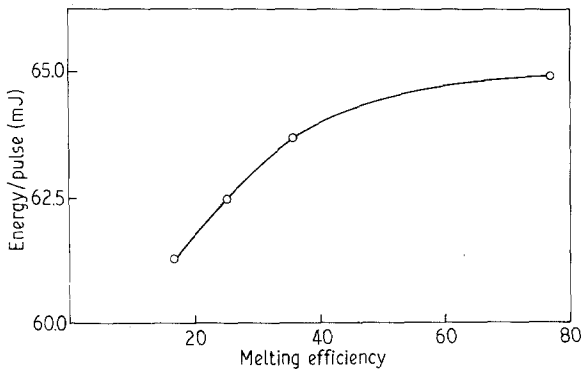

Figure 3 Melting efficiency versus laser energy for nickel, showing rapid increase in efficiency over a narrow region.

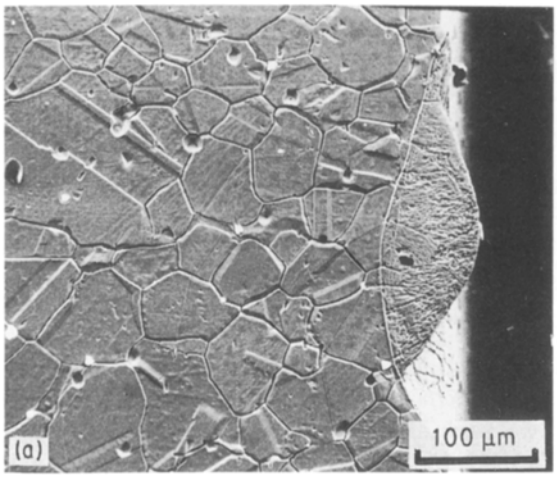

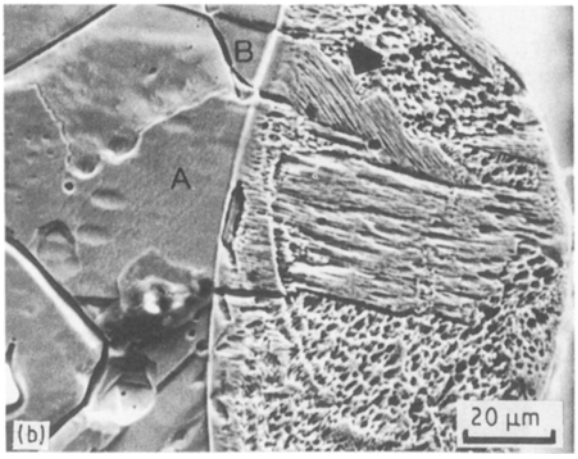

Figure 4 Scanning electron micrograph of the cross-section of a laser melted and resolidified region obtained with a laser fluence of 14.4 J cm^{-2} (total energy 63.75 mJ): (a) at low magnification revealing the grain structure; (b) at high magnification revealing the cell structure. Note that for grain B, the cell grows at an angle. As a result the grain loses out in the growth competition.

pool is evident. Fig. 4b shows a higher magnification micrograph of the substrate/resolidified pool interface. The grains are found to grow normal to the interface (opposite to the heat transfer direction). The interface is sharply delineated. The imposed growth condition tends to stifle the growth of unfavourably oriented grains of the substrate in contact with the melt. An example is shown by the arrow in Fig. 4b.

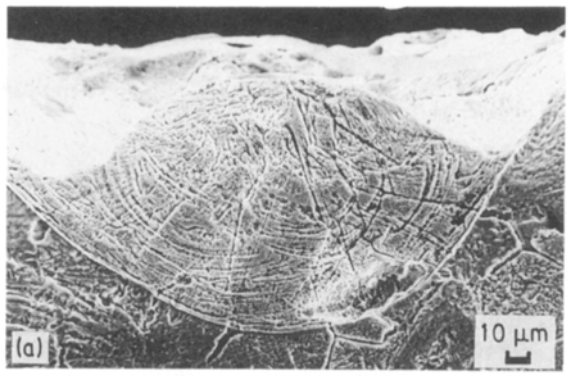

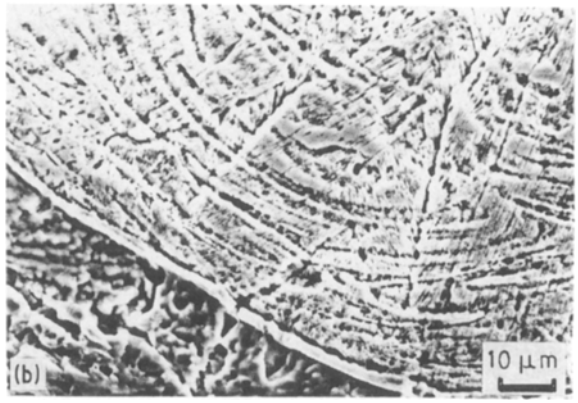

Figure 5 (a) Cross-sectional scanning electron micrograph of laser melted pool obtained with a fluence of 14.75 J cm^{-2} per pulse (total energy 65 mJ). Note the semicircular banded contrast; (b) same as above but at higher magnification. The cells are clearly revealed. Note that they are not affected by the bands.

The internal growth structure within the individual grain is revealed due to the presence of impurities which partition in front of the growing interface. Due to the rapid growth rate normally associated with laser processing, the build up of this boundary layer is expected to be rapid [7]. This and kinetic undercooling at the interface due to rapid heat transfer can lead to a destabilization of the interface in spite of the presence of a positive and high temperature gradient. The cells are elongated and in general grow normal to the interface. The average cell size is ~ 1.2 μm.

In the laser melted pools with still higher pulse energy where part of the liquid has been ejected during the processing, an additional feature in the form of bands roughly parallel to the substrate melt interface can be noticed. Fig. 5a shows the general morphology of these bands, while Fig. 5b shows the details at higher magnification. The crossing of the bands does not alter the fine cell spacings and therefore does not correspond to any effect related to the change of the growth velocity. Their appearance during the onset of metal removal suggests certain linkages between the two processes. This together with the fact that the bands are not observed towards the top of the pool points to a possible role of the stress that may develop during the drilling process. Further studies are in progress for a definitive understanding of this process.

Fig. 6 shows a cross-sectional microstructure of the laser melted nickel pool at lower energy (away from the nose of Fig. 1). The pool shape can now be

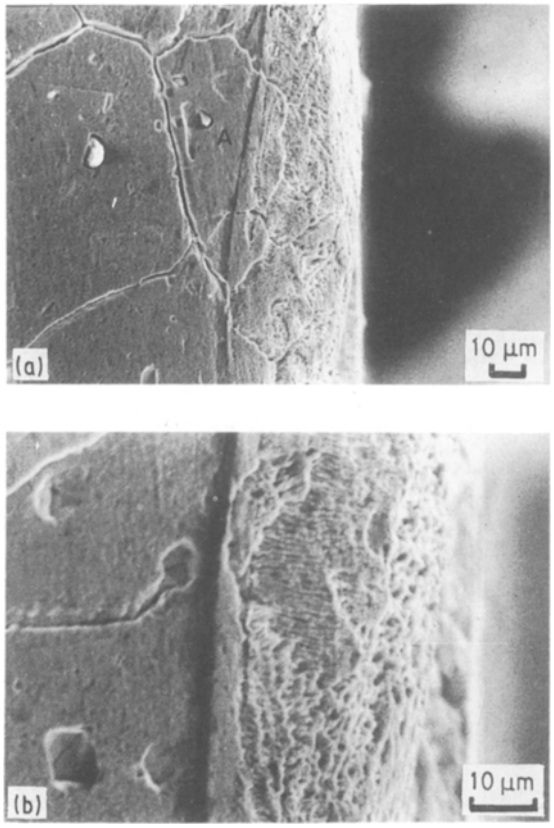

Figure 6 Cross-sectional micrograph of laser melted pool with spherical profile (average fluence 14.75 J cm^{-2}, total energy 62.5 mJ): (a) low magnification micrograph exhibiting a decrease in grain size in laser melted pool and (b) high magnification micrograph exhibiting cylindrical cells inside the grains.

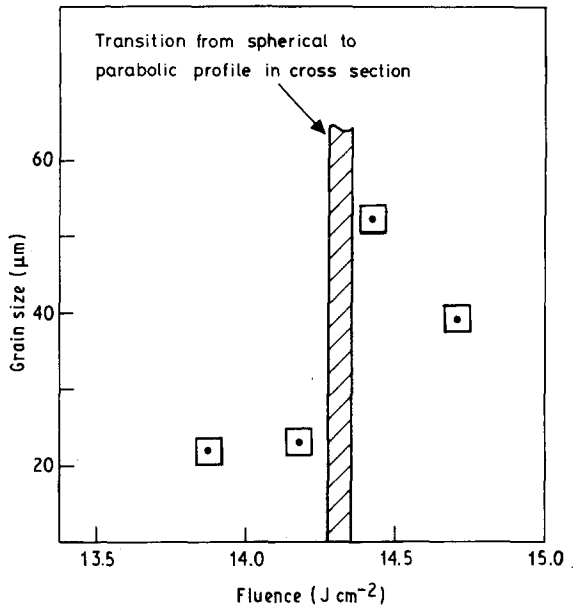

Figure 7 Grain size versus fluence highlighting a critical threshold for grain size reduction. The hatching indicates the energy range where the profile shape changes from spherical to paraboloidal shape.

approximated as a section of a sphere. The high magnification micrograph (Fig. 6b) again reveals a fine cellular structure of cylindrical shape. The average cell size of ~ 1 μm is marginally finer than that obtained in earlier high energy cases. However the most significant difference is the observation of a reduction in grain size in the resolidified pool. A comparison of Figs 5a and 6a brings out this difference unambiguously. Fig. 7 shows a plot of fluence versus grain size for four different laser energy levels. The hatching indicates the threshold for the spherical to parabolic shape change of the molten pool. The onset of drilling follows with higher fluence.

The generation of grain size finer than that of the substrate is of special interest. The resolidification of the laser melted pool normally takes place by the epitaxial regrowth of the substrate. As mentioned in the introduction, such a growth process will either retain or increase the original grain size. The decrease of grain size is difficult to explain in terms of any growth model. The chemical analysis and the observation of cells indicate the important role the impurities play during the growth process. The requirement of partitioning of these solutes will determine the maximum growth rate of the interface during the initial stage of growth. This restriction under the high heat transfer situation may lead to significant interface undercooling. Several investigators have studied the growth of nickel from undercooled melt [8–11]. One of the important findings is the observation of a transition from coarse to fine grain structure around a critical undercooling of 150 K ($\sim 0.10\ T_m$) [8, 9]. The onset of cavitation nucleation was originally proposed by Walker [8] to explain this transition.

In this respect our results of a transition from epitaxial regrowth to nucleation of fresh nickel grain is similar. In case partition requirement controls the growth, the time required for the partition of solute across the 1 μm cell is 2.5×10^{-4} s assuming a diffusivity of the order of 10^{-5} cm^2 s^{-1}. Thus a cooling rate of 10^7 K s^{-1}, which is typical of low energy microsecond pulse laser, can yield a kinetic undercooling of the same order as observed for the fine grain transition in undercooled nickel.

It is pertinent to note that no such transition could be observed for fcc copper [12] although earlier experiments with copper containing oxygen exhibited grain refinement effect [13]. In the undercooling experiments under microgravity conditions, niobium droplets did not show any grain refinement effect [14]. The evidence suggests the heterogeneous nucleation by NbO in the undercooled liquid yielding single crystal droplet. Kattamis and co-workers investigated internal growth morphologies of nickel alloys [15, 16]. These and other works on undercooling (see for example the undercooling results of Cd–Zn alloys [17]) suggest a transition from dendrites to cylindrical cells to spherical morphology with increasing undercooling. These investigators associated the onset of fine grain size with the appearance of spherical morphology. Clearly in the present case grain interiors have cylindrical cell morphology and thus do not conform to the above situation. It is more likely that cavitation aided by surface tension induced Marangoni flow may play a dominant role in the development of finer grain sizes than the substrate.

4. Conclusions

The present investigation allows us to draw the following conclusions.

1. The melting efficiency during Nd glass pulse laser interaction increases significantly with an increase in laser energy and can reach approximately 80% of the total input energy.

2. The shape of the melt pool undergoes a change from spherical to parabolic profile prior to the onset of drilling.

3. The resolidified grains have a cellular microstructure. The cells are cylindrical and grow normal to the melt–solid interface.

4. Consistent with the earlier results of undercooling a coarse to fine grain transition is observed with a decrease in the total laser energy. For nickel, it also coincides with the profile shape change threshold of input energy.

5. The microstructure during the onset of drilling exhibits a banded feature near the substrate in the resolidified pool.

Acknowledgements

The authors thank Professor C. R. K. Prasad for allowing us to use the laser facility and discussions. We also thank Dr G. Malkondaiah for help during the course of this investigations.

References

1. L. BUENE, J. M. POARTE, D. C. JACOBSON, C. W. DRAPER and J. K. HIROVONEN, *Appl. Phys. Lett.* **37** (1980) 385.
2. V. T. SWAMY, S. RANGANATHAN and K. CHATTOPADHYAY, *J. Cryst. Growth*, **96** (1989) 628.
3. C. R. PRASAD, K. KRISHNAPRASAD, M. NALLASWAMY, S. P. VENKATESHAN and A. YOGANARASIMHA, in "Laser Laboratory Report, ME–LLR–1" (Bangalore, 1978).
4. M. VON ALLMEN, *J. Appl. Phys.* **47** (1976) 5460.
5. C. M. BANAS and R. WEBB, *Proc. IEEE*, **70** (1982) 556.
6. G. M. IZMAILOVA, V. S. GALERILYUK and A. G GRIGORYANTS, *Welding Internat.* **4** (1989) 329.
7. V. G. SMITH, W. B. TILLER and J. W. RUTTER, *Can. J. Phys.* **33** (1956) 723.
8. J. L. WALKER, in "Physical Chemistry of Process Metallurgy", edited by G. R. S. Pierre (AIME, Warrendale, USA, 1961) p. 845.
9. B. CHALMERS, in "Principles of Solidification" (Wiley, New York, 1969) p. 114.
10. M. C. FLEMINGS and Y. SHIOHARA, *Mater. Sci. Engng* **65** (1984) 171.
11. T. Z. KATTAMIS and M. C. FLEMINGS, *Trans. AIME* **36** (1966) 1523.
12. B. J. JONES and G. M. WESTON, *J. Cryst. Growth* **7** (1970) 143.
13. G. L. F. POWELL and L. M. HOGAN, *Trans AIME*, **242** (1968) 2133.
14. L. L. LACY, M. B. ROBINSON and T. S. RATH, *J. Cryst. Growth* **51** (1981) 47.
15. T. Z. KATTAMIS and M. C. FLEMINGS, *Trans AIME*, **236** (1966) 1523.
16. S. SKOLIANOS, P. S. LIN and T. Z. KATTAMIS, in Proceedings of the Conference on Grain Refinement in Castings and Welds, edited by G. J. Abbaschian and S. A. David (Metallurgical Society of AIME, Warrendale, 1983) p. 97.
17. S. N. OJHA, T. R. ANANTHARAMAN and P. RAMACHANDRARAO, *J. Mater. Sci.* **17** (1982) 2644.

Received 7 January
and accepted 13 May 1991